

Characterizing Bounded Plasmas using THz Time Domain Spectroscopy

IEPC-2024-360

*Presented at the 38th International Electric Propulsion Conference
Pierre Baudis Convention Center • Toulouse, France
June 23-28, 2024*

Muhannad Eladl¹ and Mitchell L. R. Walker²
Georgia Institute of Technology, Atlanta, Georgia, 30318, USA

Abstract: THz time-domain spectroscopy (THz TDs) is a novel plasma diagnostic which measures line-averaged electron density and line-integrated electron collision frequency. THz-TDs has a unique ability to transmit through many dielectric materials, including boron nitride which is typically used as the wall material for Hall thrusters. The work presented in this paper explores this ability by measuring the properties of a plasma bounded by three types of boron nitride: M, M26, and HP, which are representative of the wall material used in many flight-grade and lab Hall thrusters. Initially, the boron nitride samples are placed in the pathway of the THz wave propagation but outside the plasma in order to investigate the claim that transmitting the wave through the dielectrics does not change the measurements made. It was found that the difference in plasma properties measured with varying RF power when compared to the case with no boron nitride was less than 7% for all three types, thus verifying this claim. The boron nitride samples are then placed inside the plasma discharge, and the properties of the bounded plasma are measured. When comparing the bounded plasma to the unbounded case, it was found that the electron density decreased by an average of ~43%. In comparison, the electron collision frequency increased by an average of ~36%. These changes are attributed to the loss in electron energy due to wall collisions. It was also found that the bounded plasma case had greater instabilities, but more investigation is required to understand the cause of this. The work presented in the paper is a first step towards applying this diagnostic to take measurements inside the discharge channel of a Hall thruster.

Nomenclature

A	=	amplitude of THz transfer function
b	=	measured THz properties
c	=	speed of light
CCP	=	capacitively coupled plasma
e	=	elementary electron charge
FWHM	=	full-width half maximum
GaAs	=	gallium arsenide
GDD	=	group delay dispersion
ICP	=	inductively coupled plasma
L	=	plasma length
m_e	=	electron mass
n_e	=	electron density
PDF	=	probability distribution function
SNR	=	signal-to-noise ratio
SWR	=	standing wave ratio
V	=	volts

¹ Graduate Research Assistant, Aerospace Engineering, meladl3@gatech.edu.

² School Chair, Aerospace Engineering, mitchell.walker@ae.gatech.edu.

x	=	plasma properties
ZnTe	=	zinc telluride
ϵ_0	=	permittivity of free space
θ	=	nuisance parameters
ϕ	=	phase of THz transfer function
ω	=	THz frequency
ω_p	=	plasma frequency
ν	=	electron collision frequency

I. Introduction

AS interest in using electric propulsion for in-space applications increases, there is a growing need to gain a better understanding of the plasma properties and processes within EP thrusters. Traditional physical probes are limited in their capability of measuring plasma properties in the near-field or discharge of the thruster due to their invasive nature, which will inherently interfere with the operation of the thruster, thus changing the properties being measured and creating uncertainty in the reliability of the results. Many non-invasive diagnostics, such as LIF and Thomson Scattering, are used to measure plasma properties. Still, most of these techniques require an optical line of sight, thus limiting where the measurements can be taken¹. THz Time Domain Spectroscopy (THz-TDs) is a novel plasma diagnostic technique with the capability of transmitting through many dielectric materials including boron nitride, the wall material typically used to bound plasmas within the discharge of Hall thrusters. This capability gives the diagnostic the potential to non-invasively measure plasma properties, specifically electron density and electron collision frequency, within the discharge channel of a Hall thruster¹.

The purpose of this paper is to test the efficacy of THz-TDs in measuring the properties of an RF ICP plasma bounded by boron nitride. A previous experiment² showed that plasma properties can be measured through boron nitride. However, the experimental setup led to some ambiguity in the neutral pressure of argon within the discharge and, hence, the resulting measured properties. The works described in this paper take a slightly different approach to the setup to avoid this issue as well as experimentally verify some of the claims made in previous works^{1,2} to further add confidence in the use of THz-TDs to measure bounded plasma properties.

The proposed work consists of two parts. The first part is verifying that transmitting THz through boron nitride does not affect the measurement of the plasma properties. This will be achieved by taking measurements with and without boron nitride in the path of the propagating THz wave but outside the plasma to ensure that the boundary itself is not affecting the plasma. The second part of the proposed work is to place the boron nitride in the plasma and measure the effect of the existence of a boundary will have on the plasma properties. The manuscript is organized as follows. Section II describes the experimental setup, providing a brief overview of the operating principles behind THz-TDs and a description of the RF plasma cell. Section III presents the results of the experiment and their implications. Section IV summarizes the conclusions that can be drawn from the results and possible future work.

II. Experimental Setup

A. THz TDs

THz-TDs is a spectroscopic technique that relies on the generation and detection of pulsed THz radiation¹. THz radiation is generated on a pico-second time scale using a photoconductive antenna, steered into the plasma, and then measured using an electro-optical crystal. As the THz pulse propagates through the plasma, its amplitude and phase change with the level of change depending on the refractive index of the plasma, which is a function of the plasma properties. By measuring a reference THz pulse through the air and a sample pulse through the plasma, it can be shown, under the Lorentz plasma assumptions, that the amplitude (A) and phase (ϕ) of the resulting transfer function can be related to the plasma properties as follows¹:

$$A(\omega) = \left(\frac{1}{r}\right) \exp \left[-\frac{\omega L}{c} \sqrt{-\frac{1}{2} \left(1 - \frac{\omega_p^2}{\omega^2 + \nu^2}\right) + \frac{1}{2} \sqrt{\left(1 - \frac{\omega_p^2}{\omega^2 + \nu^2}\right)^2 + \left(\frac{\omega_p^2 \nu}{\omega[\omega^2 + \nu^2]}\right)^2}} \right] \quad (1)$$

$$\phi(\omega) = \phi_2 \omega + \frac{\omega L}{c} \left[\frac{1}{2} \left(1 - \frac{\omega_p^2}{\omega^2 + \nu^2}\right) + \frac{1}{2} \sqrt{\left(1 - \frac{\omega_p^2}{\omega^2 + \nu^2}\right)^2 + \left(\frac{\omega_p^2 \nu}{\omega[\omega^2 + \nu^2]}\right)^2} - 1 \right] \quad (2)$$

$$\omega_p = \sqrt{\frac{n_e e^2}{\epsilon_0 m_e}} \quad (3)$$

Where, ω is the THz wave frequency, L is the plasma length, c is the speed of light, ω_p is the plasma frequency, ν is the electron collision frequency, n_e is the electron density, e is the elementary charge of an electron, m_e is the mass of the electron, ϵ_0 is the permittivity of free space, r is the amplitude correction factor, and φ_2 is the phase correction factor. The details of the derivation for these relationships can be found in Ref. 1. Hence, by comparing the reference and sample THz pulses, the line-averaged electron density and line-integrated electron collision frequency can be measured.

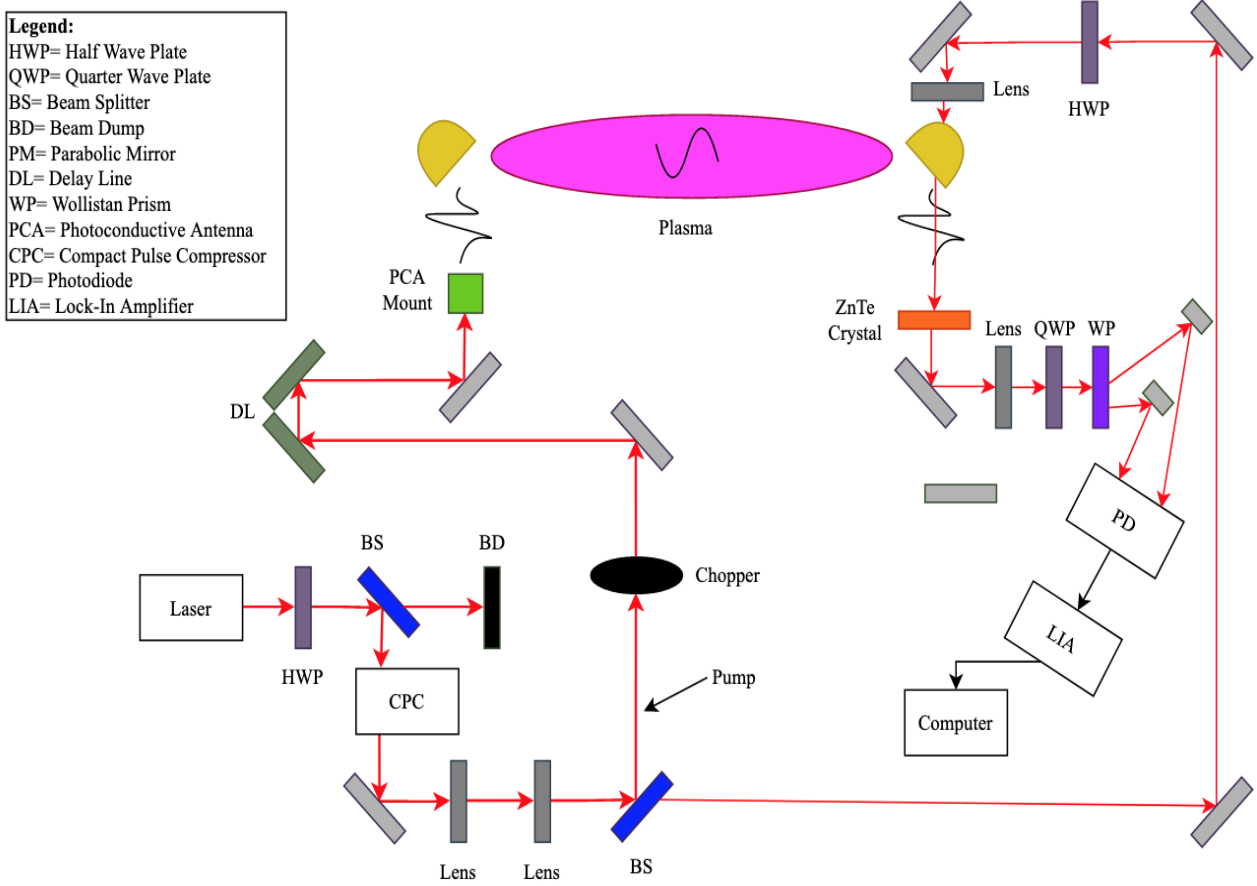


Figure 1. THz TDs setup schematic

Fig. 1 shows a schematic for the THz setup used for this experiment. The setup uses a Coherent Vitara-T-HP 1.2 W Ti:Sapphire laser with an 800 nm central wavelength and a temporal width of 20 fs FWHM. The THz is generated using a GaAs photoconductive antenna and detected using a ZnTe crystal. The photoconductive antenna consists of a gold electrode layered on top of a GaAs semiconductor substrate. A 15-V DC bias is applied to the gold electrode. When the laser is pulsed onto the antenna, electrons are excited out of the ground state to a conducting state and are accelerated by the applied bias, generating a current before de-exciting back into the ground state. This pico-second time scale pulsed current generates radiation in the THz frequency range. The ZnTe crystal detects the THz through the Pockels effect¹. When the laser and THz pulses are incident onto the crystal at the same time, the polarization of the laser pulse is rotated due to the non-linear electro-optical properties of the ZnTe crystal. The degree of rotation of the polarization of the laser pulse is proportional to the E-field of the THz wave. Low GDD optics are used to ensure that the laser pulse temporal width is kept below 100fs. In order to minimize noise and hence improve the SNR, the setup incorporates a 1-kHz optical chopper and a lock-in amplifier. Ref 1. provides more details on the optical components used in the setup.

B. RF Plasma

An argon radio frequency inductively coupled plasma (RF ICP) serves as the testbed for this investigation. The testbed consists of a custom-made quartz tube cross discharge chamber with a 2-inch outer diameter, 0.2-inch wall thickness, 18" length and 10" width. The discharge chamber length ends in two Z-cut crystalline quartz viewports (Torr Scientific BKVPZ50NQZ), through which the THz wave passes. Z-cut quartz is chosen for its high transmissibility in the THz regime. The discharge chamber has a vacuum base pressure of 25 mTorr. A MKS GE50A013102SMV020 mass flow controller with a 100 sccm full-scale ± 1 sccm, is used to control the neutral argon pressure inside the chamber. The pressure in the chamber is measured using a Kurt J. Lesker KJL 275807LL convection pressure gauge with an uncertainty of $\pm 10\%$ of the reading. The operating pressure is 1 Torr argon for all cases. The RF power is generated by a Materials Science, Inc. RF-3-XIII 13.56 MHz RF power supply and coupled into the discharge by a three-turn copper antenna wrapped around the discharge. A Kessler AT-Auto RF impedance matcher is used to ensure that the standing wave ratio (SWR) is kept at a value of 1.05. A Telepost Inc. LP-100A wattmeter is used to measure the power with an uncertainty of ± 1 W and the SWR with an uncertainty of ± 0.01 . The RF system can have some drift or instability in the power output and standing wave ratio during startup, as such measurements are taken 10 minutes after initial startup to ensure all drift and instabilities have settled. Fig. 2 shows the testbed, and Fig. 3 shows the RF electrical schematic.

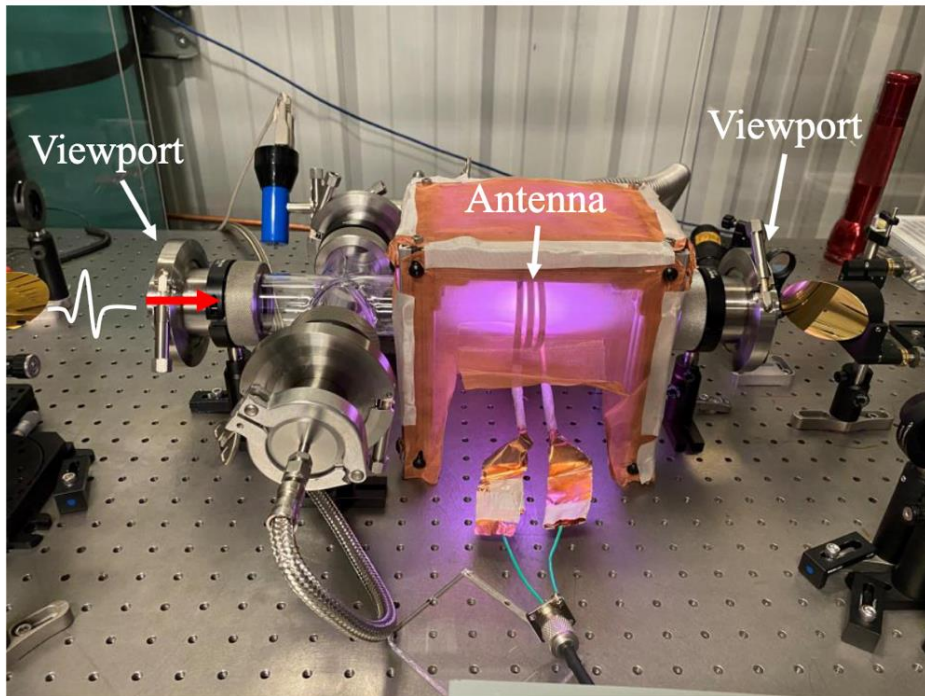


Figure 2. RF ICP testbed¹

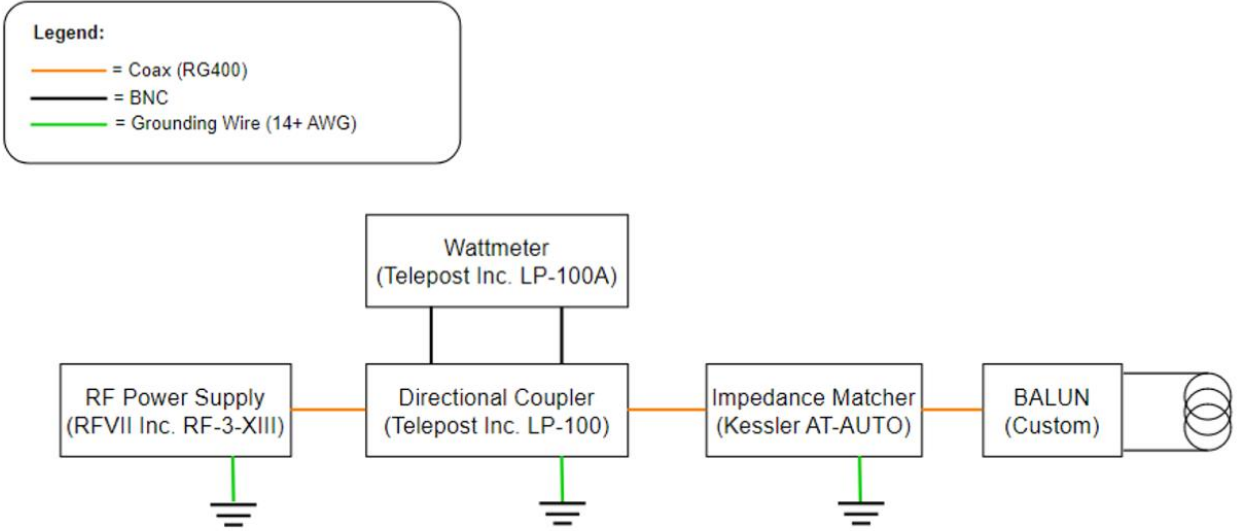


Figure 3. RF system electrical block diagram

III. Results and Discussion

A. Bayesian Analysis Overview

The data collected for this investigation is analyzed by employing a Bayesian framework, in which each variable is treated as a random variable with a distribution instead of a specified value. This framework allows for a self-consistent quantification of the uncertainty of the measured properties as well as accounts for measurement artifacts that arise from delay line drift and refraction that can distort the resulting plasma properties, specifically the electron collision frequency³. The Bayesian framework calculates the posterior PDF, $p(\mathbf{x}|\mathbf{b})$, which represents the distribution of the plasma properties (\mathbf{x}), given the measured values of the THz transfer function amplitude and phase, summarized as the variable \mathbf{b} . The posterior PDF is calculated using Bayes theorem:

$$p(\mathbf{x}, \boldsymbol{\theta}|\mathbf{b}) = \frac{p(\mathbf{x}, \boldsymbol{\theta})p(\mathbf{b}|\mathbf{x}, \boldsymbol{\theta})}{p(\mathbf{b})} \quad (4)$$

Where $\boldsymbol{\theta}$ is the nuisance parameters, which are parameters that are involved in Eqs. (1,2) and are treated as random variables, but whose final values are not of interest to the experiment. For this experiment, the nuisance parameters are the length of the plasma (L) and the phase and magnitude correction factors (φ_2, r respectively). There is a total of five random variables (plasma properties and nuisance parameters) analyzed for this work. However, the framework described here is robust and the same method can be applied to experiments with more variables. $p(\mathbf{x}, \boldsymbol{\theta})$ is the priori PDF, which incorporates any known information about the plasma before taking measurements¹. $p(\mathbf{b}|\mathbf{x}, \boldsymbol{\theta})$ is the likelihood PDF, which represents the distribution of the THz properties given a set of plasma and nuisance parameters. $p(\mathbf{b})$ is the evidence PDF, whose purpose is to normalize the posterior PDF to have an integral of unity. Details on the computational scheme used to calculate each of the PDFs can be found in Ref. 3.

Once the posterior PDF is calculated the most probable value of each plasma property is defined as the mean of their respective distribution, while the associated uncertainty is defined as $\pm 2\sigma$, where σ is the standard deviation of each distribution. Calculating the complete PDF is computationally expensive and very time-consuming. Instead, the posterior PDF is numerically sampled to create a Markov chain. The sampling process is iterative, with each iteration doubling the number of samples taken until changes in the mean of the Markov chain between iterations converge to zero within some tolerance, chosen to be $\pm 0.5\%$ for this work. At this point, the Markov chain is assumed to be representative of the true posterior distribution, and the mean and standard deviation of the chain are approximately the same as the posterior PDF. Details on the mathematics behind the sampling method employed can be found in Ref. 1.

B. Boron Nitride Transmission Verification Test

In order to verify that transmitting the THz wave through boron nitride does not affect the resulting plasma properties, measurements are taken with boron nitride placed outside the plasma discharge but still in the pathway of the THz wave propagation. Three grades of boron nitride are tested: HP, M, and M26. M and M26 boron nitride are representative of flight-grade materials, while HP is often used with lab thrusters¹. Each boron nitride sample is machined into a circular disk with a 1.7” diameter and 0.1” thickness. Fig. 4 shows a schematic for the setup with the BN sample in the THz pathway.

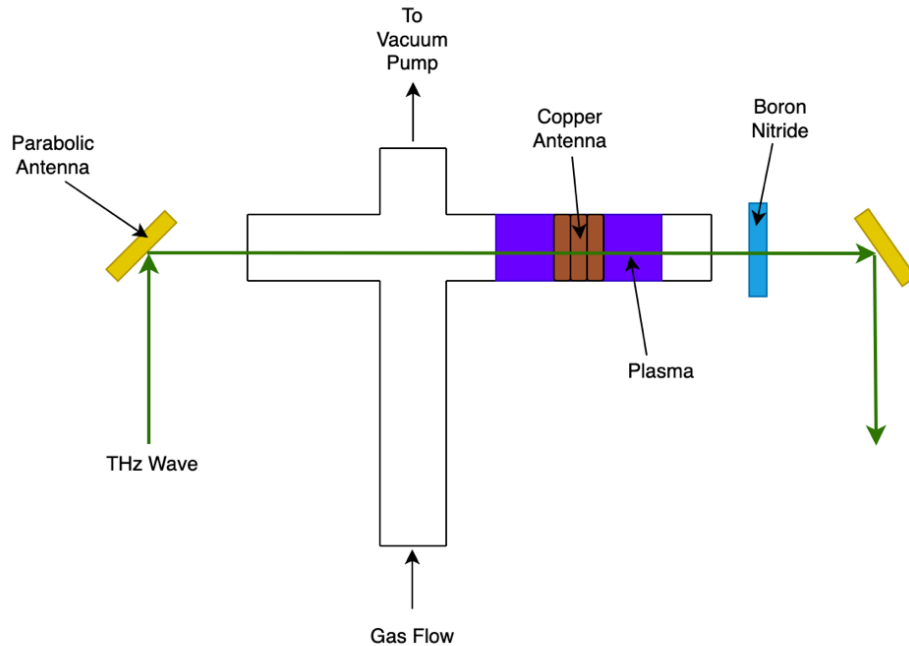


Figure 4. Schematic of test setup with BN in the THz pathway

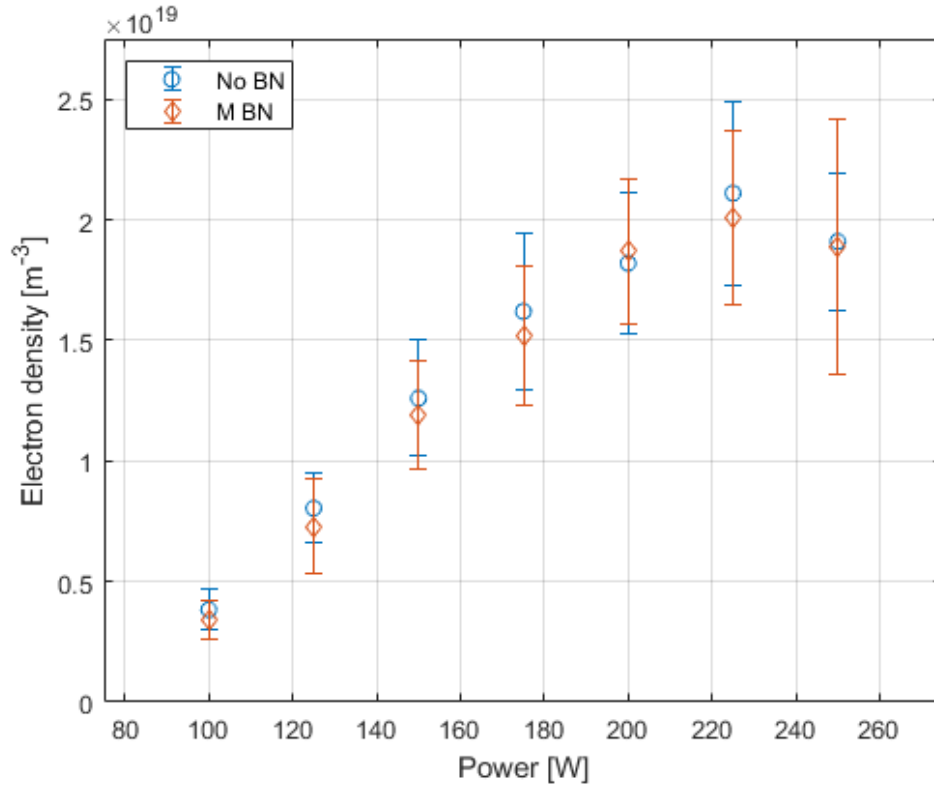
For each case, the plasma properties are measured for varying RF powers in the range of 100-250 W with 25 W increments. Comparisons between the plasma properties measured with each type of boron nitride in the propagation path and no boron nitride in the propagation path are plotted in Fig. 5-6. It is important to note that a new measurement (plasma off) needs to be taken with each type of boron nitride in the propagation path. In all three cases, the measurements with and without the boron nitride agreed within the uncertainties of the measurement. Table 1 presents the mean difference between each BN case and no BN, as well as the mean uncertainty for each case.

Table 1. Plasma properties for each type of BN in the measurement pathway with respect to no BN.

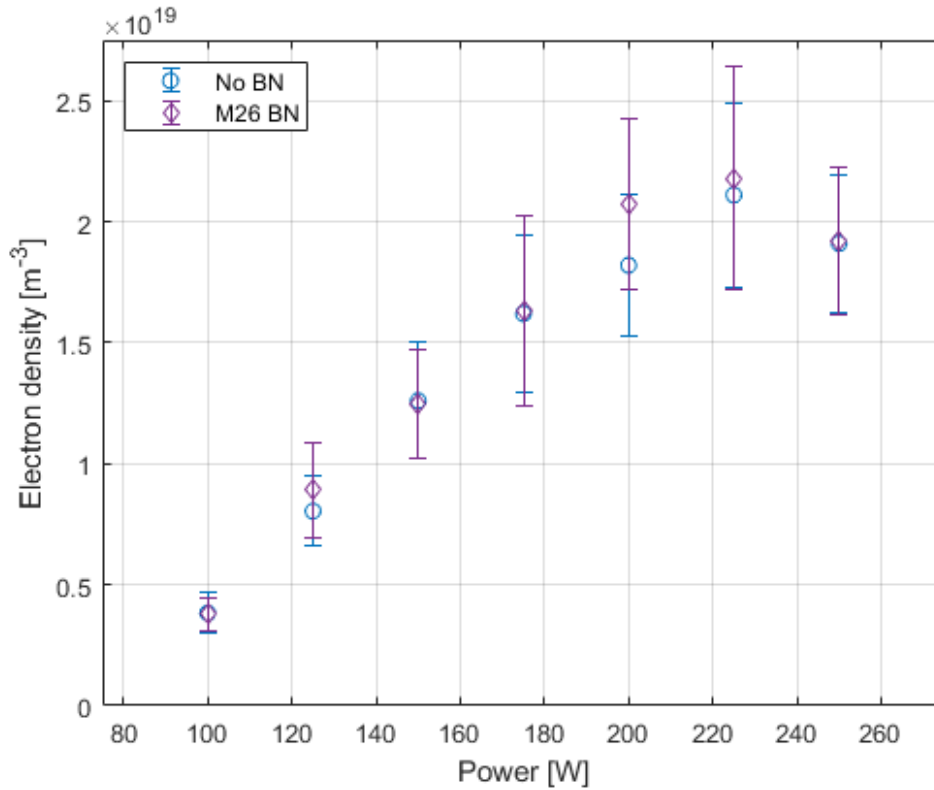
BN Type	Mean Electron Density Difference [%]	Mean Electron Density Uncertainty [%]	Mean Collision Frequency Difference [%]	Mean Collision Frequency Uncertainty [%]
M	5.8	21	6.1	26
M26	4.5	21	7.9	25
HP	6.3	23	7.4	26

In all three BN cases and the no BN case, the trends in the electron density and collision frequency are the same. The electron density is found to increase with RF power before starting to flatten off at ~ 200 W. Similar trends have been observed in other experiments using OES⁴ and Langmuir probes⁵, although the saturation in electron density typically is not observed until much higher powers. This could be due to the fact that the discharge chamber used for this work is much smaller than those in the cited works, and hence a much smaller volume of gas is being ionized, as well as the larger role that skin effects will have in the coupling between the antenna and the plasma.

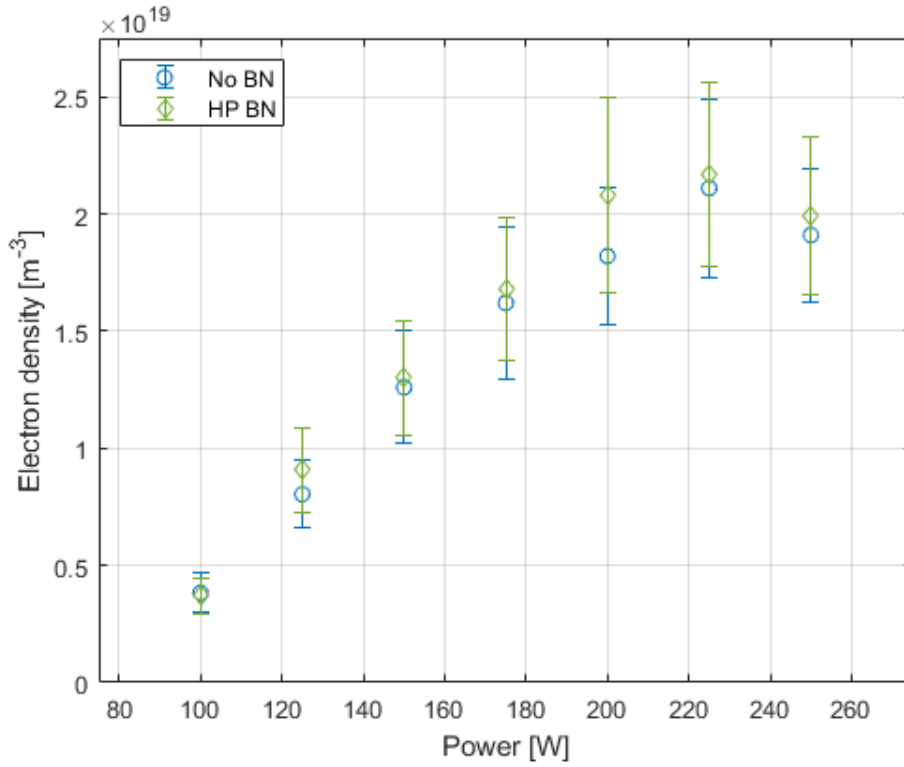
The collision frequency is found to decrease with RF power until flattening off at ~ 175 W. This differs from the THz measurements of collision frequency presented in Ref. 1, which showed a slight decrease in collision frequency with increasing RF power. No other published data that investigates electron collision frequency as a function of RF power for an ICP was found. However, previous experimental and modeling work has found that electron-neutral collisions are the dominant collision for low-temperature ICP plasmas^{6,7}. Given that the neutral gas pressure is kept constant, as the electron and plasma densities increase the neutral density will decrease. A decrease in the neutral density coupled with the electron temperature remaining approximately constant⁸ would lead to a decrease in electron-neutral collisions and hence overall electron collision frequency which matches the THz results.



a)

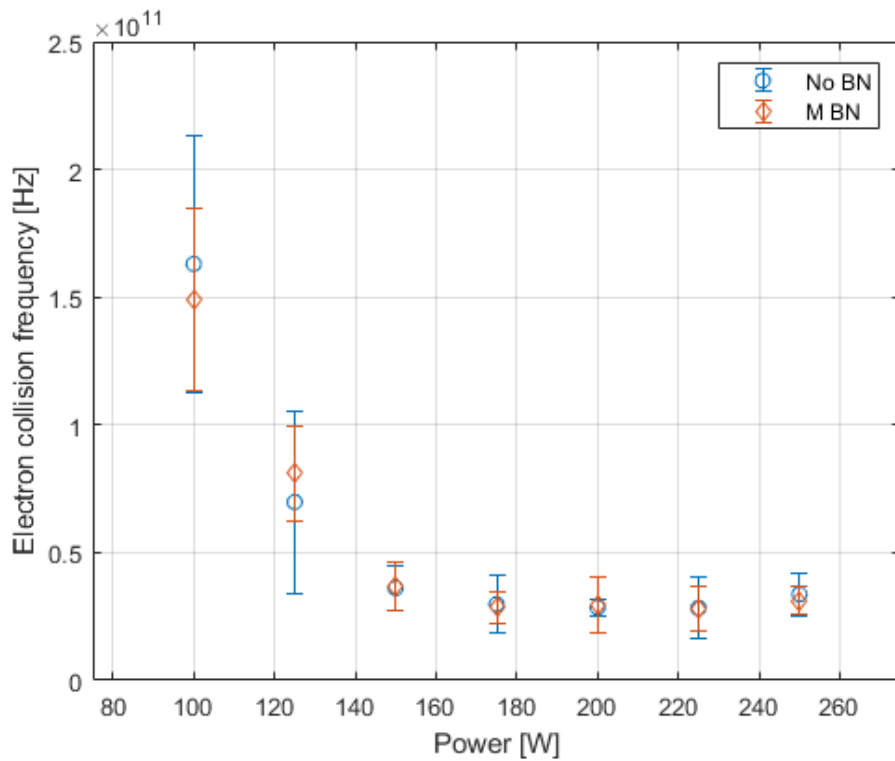


b)

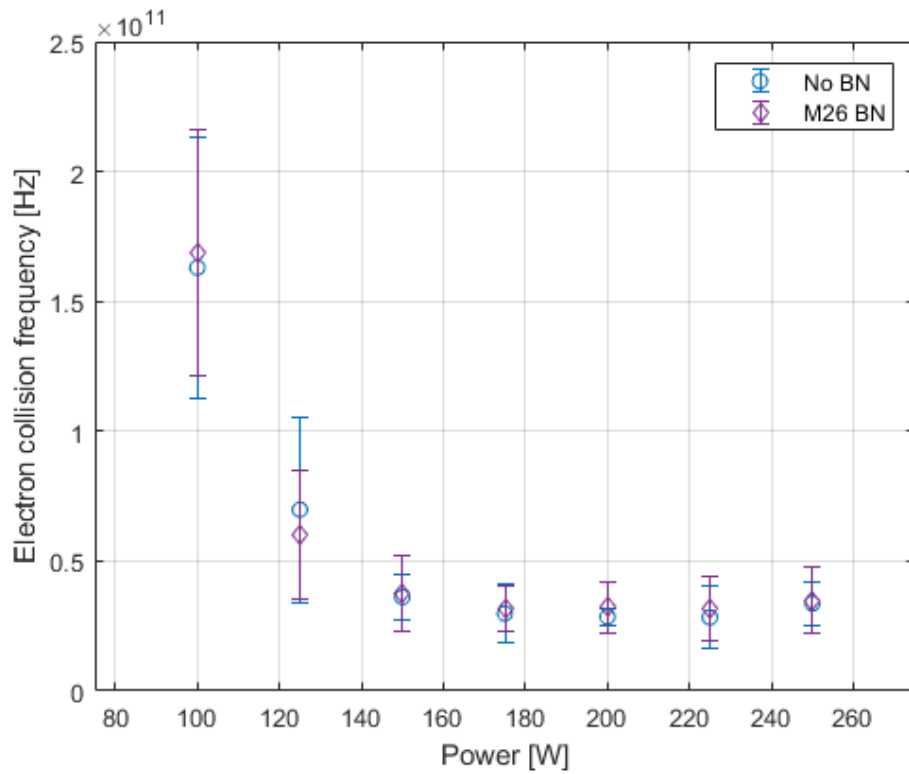


c)

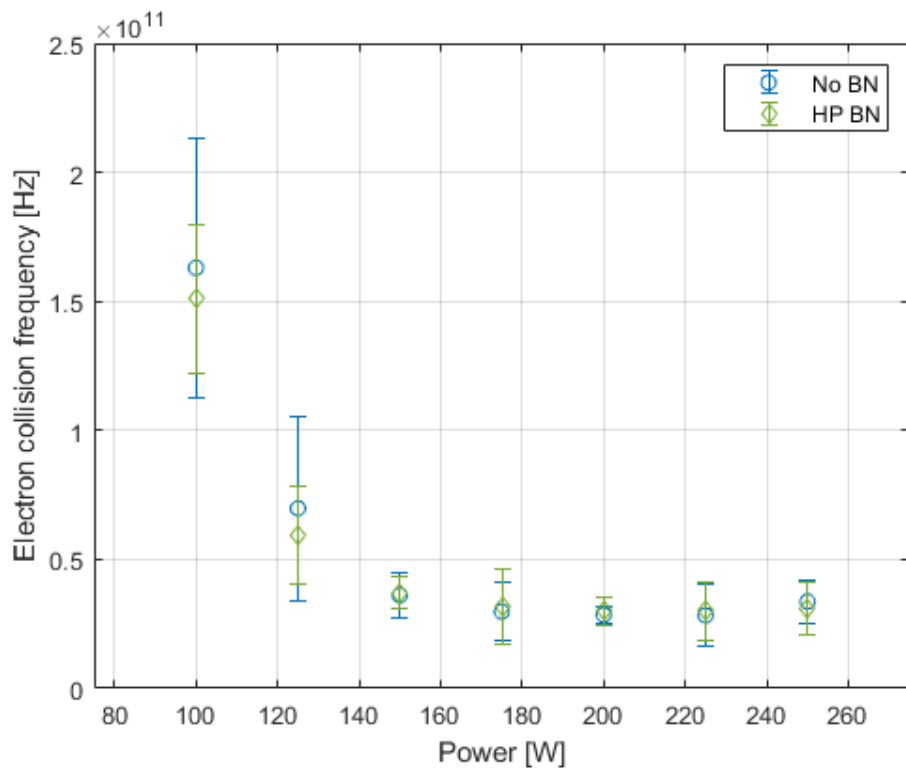
Figure 5. Electron density as a function of power for no BN in the THz pathway and a) M BN b) M26 BN and c) HP BN in the THz pathway



a)



b)



c)

Figure 6. Electron collision frequency as a function of power for no BN in the THz pathway and a) M BN b) M26 BN and c) HP BN in the THz pathway

C. Bounded Plasma Test

The purpose of the second test is to measure how bounding the plasma with a dielectric would change the plasma properties. Similar to the first test, measurements are taken for a range of RF powers from 100-250 W in 25 W increments. The plasma is bounded from only one side to ensure that the gas flow to the plasma region is not impeded hence ensuring there is no ambiguity in the neutral pressure. The BN samples are placed 1" from the edge of the antenna edge. Due to mechanical issues, only data for the plasma bounded by M and M26 BN is measured.

Placing the BN inside the discharge led to visual changes in the plasma, as can be seen in Fig. 7. The ICP region of the plasma is smaller, going from ~3" without the BN to ~1" with the BN. There is also a change in the color of the plasma, shifting from a pink/purple color for the unbounded case to white for the bounded case. Having the BN inside the discharge also leads to instabilities in the plasma seen as visual oscillations in the plasma itself as well as fluctuations of $\pm 10\%$ in the RF power and SWR. It is important to note that the ICP is always accompanied by a dim capacitively-coupled plasma (CCP) region further away from the antenna. Given that this region is very dim and CCP plasma properties are at least an order of magnitude smaller than ICP properties⁴, the contribution of this region to the line-averaged and line-integrated measurements is assumed to be negligible, and only the length of the ICP region is considered. For the bounded plasma, the CCP region is larger and brighter than the unbounded plasma. The CCP region is still much dimmer than the ICP region, and hence only the length of the ICP region is considered. However, it is important to note the slight additional ambiguity in defining the plasma length for the bounded plasma case. The observed visual changes to the plasma when bounded are the same for both the M and M26 BN cases.

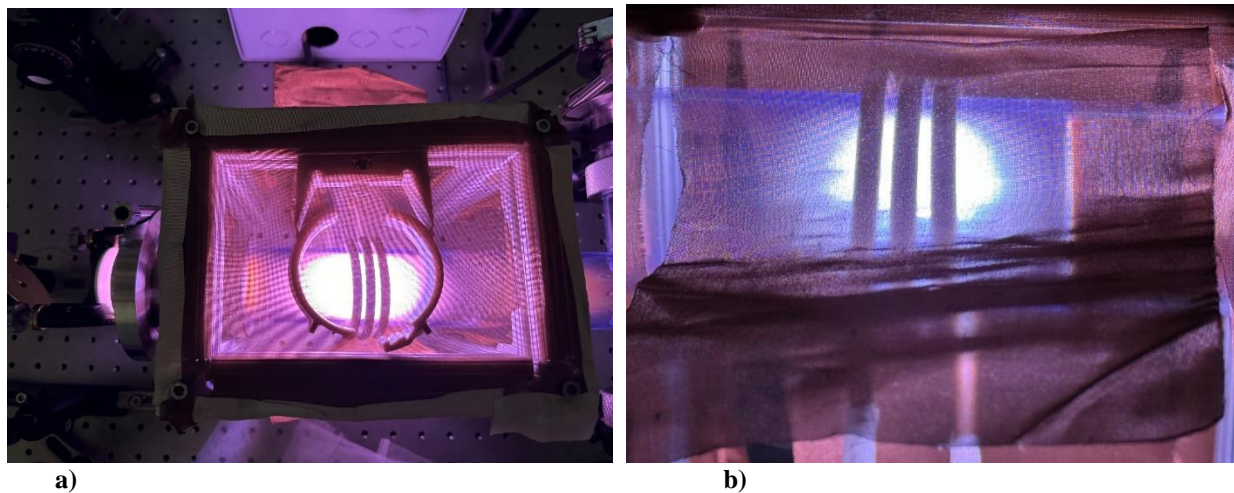


Figure 7. Visual comparison of a) unbounded plasma and b) plasma bounded by M26 BN at 200 W

The plasma properties for the bounded and unbounded cases are presented in Fig. 8. For the bounded plasma cases, the electron density had a mean decrease of ~43%, and the electron collision frequency had a mean increase of ~36% when compared to the unbounded case. A previous experiment investigating the effect of having a dielectric tube immersed in an ICP found that near the dielectric, within 2", the electron density dropped by a mean of ~51%⁹, which is commensurate with the THz results. Given the dominant collision type is electron-neutral, the decrease in electron/plasma density and, hence, an increase in neutral density would lead to an increase in collision frequency, as seen in the results. It is important to note that the collision frequency is measured in the direction of the polarization of the E-field of the THz wave, which is perpendicular to the direction of propagation of the wave. Therefore, collisions with the boundary itself, which are normal to the propagation direction of the THz wave, are not included in the measurements. One potential reason for the change in plasma properties could be due to the loss of energy when electrons collide with the boundary, which would, in turn, decrease the number of collisions that lead to ionization. This would explain why, in Ref 9, the decrease in the plasma density is limited to the vicinity of the dielectric, with the measured electron density further than 2" experiencing a mean decrease of only 8%. Further investigation of how the plasma properties will change with the BN boundary placed at different locations relative to the antenna is needed to verify whether the same trends will be seen with this setup. However, the cause of the instability in the plasma and RF system is still not well understood. It would also be interesting to repeat the experiment with different dielectrics to see what role, if any, secondary electron emission would have on the plasma properties

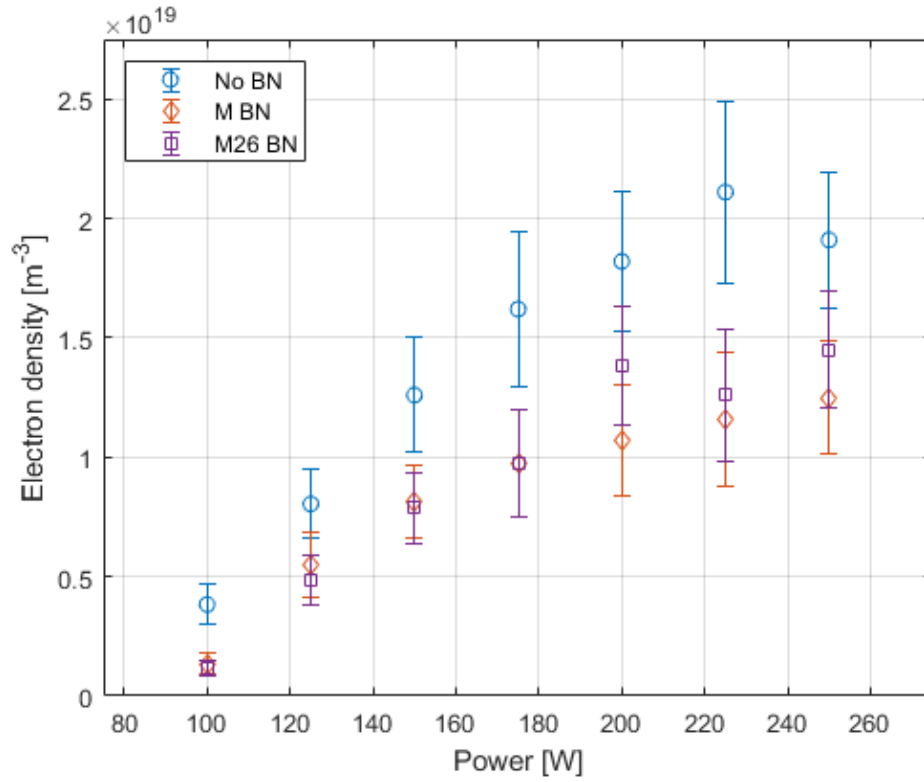


Figure 8. Electron density as a function of power for bounded and unbounded plasmas

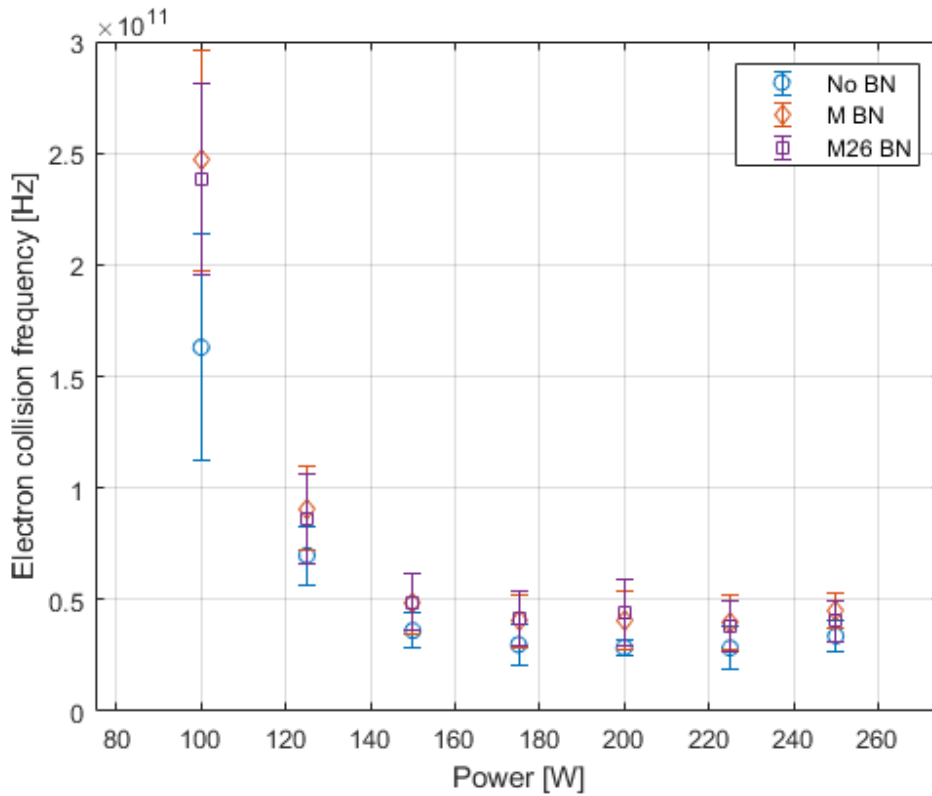


Figure 9. Electron collision frequency as a function of power for bounded and unbounded plasmas

IV. Conclusion

This paper investigates the use of THz TDs as a diagnostic for measuring properties of plasmas bounded by boron nitride. By placing different types of BN in the pathway of the THz propagation but outside the plasma, we verified that the presence of the dielectric in the measurement line of sight does not affect the resulting measurements. The effect of bounding the plasma with boron nitride was also investigated and it was found that the electron density decreased while the electron collision frequency increased. Further investigation is required to gain a better understanding of the reason for these changes as well as the cause of the instabilities that are observed for the bounded plasma case. The work presented in this paper increases the confidence in THz as a diagnostic with the ability to measure properties of plasmas whose optical line of sight is blocked by dielectrics typically used in electric propulsion thrusters, thus taking a further step towards applying this diagnostic to EP devices.

References

- ¹Brown, N. P., “Development and Evaluation of Terahertz Time Domain Spectroscopy for Electric Propulsion Plasma Diagnostics,” Ph.D. Dissertation, Aerospace Dept., Georgia Institute of Technology, Atlanta, GA, 2020
- ²Brown, N. P., Eladl M., Steinberg A., Deibel J., and Walker, M. L. R., “Noninvasive THz-TDs Measurements of Plasma Bounded and Optically Shielded by Hall Thruster Wall Material,” *Plasma Sources Science and Technology*, Vol. 30, 29 July, 2021.
- ³Brown, N. P., Grauer, S. J., Deibel, J. A., Walker, M. L. R., and Steinberg, A. M., “Bayesian framework for THz-TDs plasma diagnostics,” *Optics Express*, Vol. 29, No. 4, 15 Feb., 2021.
- ⁴Yoon, M. Y., Yeom, H. J., Kim, J. H., Chegal, W., Cho, Y. J., Kwon, D., Jeong, J., and Lee, H., “Discharge Physics and Atomic Layer Etching in AR/C₄F₆ Inductively Coupled Plasmas with a Radio Frequency Bias,” *Physics of Plasmas*, Vol. 28, 18 Feb., 2021.
- ⁵Kim, J., and Chung, C., “Effect of Electron Kinetics on Plasma Density in Inductively Coupled Plasmas Using a Passive Resonant Antenna,” *Physics of Plasmas*, Vol. 27, 21 May, 2020.
- ⁶Kolobov, V., and Godyak, V., “Electron Kinetics in Low-Temperatures Plasmas,” *Physics of Plasmas*, Vol. 26, 4 June, 2019.
- ⁷Lee, H., “A Brief Review of Electron Kinetics in Radio-Frequency Plasmas,” *Applied Science and Convergence Technology*, Vol. 28, 24 July, 2019.
- ⁸Lee, H., Seo, B. H., Kim, J. H., Seong, D. J., Oh, S. J., Chung, C. W., You, K. H., and Shin, C., “Evolution of Electron Temperature in Inductively Coupled Plasma,” *Applied Physics Letters*, Vol. 110, 6 Jan., 2017.
- ⁹Bi, Z., Hong, Y., Lei, G., Wang, S., Wang, Y., and Liu, D., “Influence of a Centered Dielectric Tube on Inductively Coupled Plasma Source: Chamber Structure and Plasma Characteristics,” *Chinese Physics B*, Vol. 26, No. 7, 6 June, 2017.